Int. J. Electrochem. Sci., 9 **(2014)** 2518 - 2534

International Journal of
ELECTROCHEMICAL
SCIENCE
www.electrochemsci.org

Carbon-Supported Manganese Dioxide as Electrode Material For Asymmetric Electrochemical Capacitors

Ilona Acznik[1,*], *Katarzyna Lota*[1], *Agnieszka Sierczynska*[1], *Grzegorz Lota*[1,2]

[1] Institute of Non-Ferrous Metals Division in Poznan, Central Laboratory of Batteries and Cells, Forteczna 12, 61-362 Poznan, Poland
[2] Institute of Chemistry and Technical Electrochemistry, Poznan University of Technology, Piotrowo 3, 60-965 Poznan, Poland
[*]E-mail: ilona.acznik@claio.poznan.pl

Received: 13 December 2013 / *Accepted:* 17 January 2014 / *Published:* 2 March 2014

Composites of carbon nanotubes and activated carbon with manganese dioxide (MN MnO_2, DN MnO_2, AC2 MnO_2) were chosen as positive electrodes and activated carbon (AC1) with well-developed surface area as negative electrode. C/MnO_2 composites were prepared with various C:MnO_2 ratio (c.a. 30, 50 and 60% of MnO_2). The electrochemical performance of symmetric and asymmetric capacitors was studied in two and three electrode configuration, using 1M Na_2SO_4 aqueous solutions as electrolyte. The capacitance properties were studied by cyclic voltammetry, galvanostatic charging/discharging and electrochemical impedance spectroscopy. The asymmetric cell composed of composite AC2 MnO_2 3 gave the most preferred capacitance in the extended voltage range of 1.7 V at the level 142 F g^{-1}, however, the capacitor with MN MnO_2 3/ AC1 operating at a voltage of 1.7 V reached energy density above 20 Wh kg^{-1}. Very good stability during 5000 cycles was obtained for composites charged to 1.1 V (MN MnO_2 3) and 1.2 V (MN MnO_2 2). The capacitance of these systems has been retarded at around 110 F g^{-1} at a load current density 2 A g^{-1}. Increase of the operating voltage of the capacitor MN MnO_2 3/ AC1 from 1.2 V to 1.7 V, has initially contributed to increase in capacitance, although after 5000 cycles significant capacitance fade, i.e. from ca. 150 F g^{-1} to ca. 70 F g^{-1} was observed.

Keywords: Asymmetric supercapacitors, manganese dioxide, electrode materials, aqueous electrolytes, electrochemical stability window.

1. INTRODUCTION

Electrochemical capacitors (ECs), which are currently one of the most popular energy storage devices, have raised interest due to such advantages as, high power density, long cycle life, and very

short charging/discharging times [1-3]. It is believed that ECs can bridge the performance gap between the energy density of battery and high power density offered by conventional dielectric capacitor [4]. They are used as an auxiliary source of energy, especially in applications requiring high peak of power. To expand the range of applications their energy density should be improved. The efficiency of ECs is determined mainly by the electrochemical properties of the electrode material, but also the electrolyte plays an important role. However, most research is focused on the development of new electrode materials. An example of materials with pseudocapacitive behavior arising from redox reactions are transition metal oxides. This group includes MnO_2 which is a promising electrode material due to such advantages as low cost, nontoxity, environmental friendliness and good electrochemical properties. Theoretically, the capacitance value of MnO_2 resulting from Faraday's law can reach up to 1370 F g^{-1} ($Mn^{4+} \rightarrow Mn^{3+}$), however low reversibility of oxidation/reduction processes significantly limits their use in practice. In addition, the low conductivity of pure MnO_2 as an electrode material results in poor propagation of electric charge in the material thus reducing the capacitance [5]. For improving the conductivity and to increase the specific capacitance, ongoing researches are focused on the development of the composite electrode materials formed from MnO_2 and various carbon materials [6-9].

Given the charge storage mechanism, it can be distinguish two types of electrochemical capacitors. One of them is based on the electric double layer formed on the interface of the electrolyte and electrode with well-developed surface area, as a result of the electrostatic attraction of ions contained in the electrolyte. The second type uses a fast and reversible redox reactions (Faraday reactions), giving the so-called pseudo-capacitance [1,10,11]. The use and combination of both mechanisms constitutes interesting alternative giving the hybrid system that offers high energy (pseudo-capacitance) and high power (electrical double layer) in the same cell [12]. In addition, the asymmetric design reaches outstanding performance by extend the operating voltage window of aqueous electrolytes beyond the thermodynamic limit, leading to significantly higher specific energy than symmetric ones using aqueous electrolytes [13].

In this work, composites of carbon nanotubes/ manganese dioxide and activated carbon/ manganese dioxide have been chosen as positive electrodes and activated carbon with well-developed surface area as negative electrodes. MnO_2 composites were synthesized by a simple method of precipitation from solution, whereas activated carbon labeled as AC1, was the result of carbonization of lignin and KOH activation. The resulting materials were characterized physicochemically and electrochemically. In the initial stage of electrochemical tests, composite materials have been examined in symmetric configuration, whereas essential purpose of the study was to examine them as positive electrodes of asymmetrical capacitors in aqueous electrolyte.

Manganese dioxide was selected as an environment friendly component of electrode material. Its hydrated form is a promising material due to its pseudo-capacitive behavior according to the following reaction [14]:

$$MnO_x(OH)_y + \delta e^- + \delta H^+ \leftrightarrow MnO_{x-\delta}(OH)_{y-\delta}$$

It has already been proved that this material due to its electrochemical stability in the positive range of potentials plays a significant role as an good electrode material in supercapacitors [15-18].

2. EXPERIMENTAL

2.1 Materials preparation

The composite materials built of carbon skeleton and manganese dioxide (MnO_2) were synthesized in a gradual reaction of potassium permanganate (0.1 M $KMnO_4$) with ethyl alcohol (C_2H_5OH). For this purpose, commercially available carbons were used, i.e. activated carbon Norit GSX (Alfa Aesar) and two size of multi-walled carbon nanotubes – O.D. 7-15 nm/ length 0.5-200 μm (Aldrich) and O.D. 110-170 nm/ length 5-9 μm (Aldrich). The resulting composite materials differ in the percentage content of MnO_2. For comparison, pure manganese dioxide was also produced.

Activated carbon AC1 was prepared by carbonization of commercial lignin (Aldrich) and then activated in KOH with a C:KOH ratio of 1:4.

2.2 Physicochemical characterization

The morphology of source and synthesized materials was characterized by X-ray diffraction (XRD), scanning electron microscopy (SEM EVO®40 ZEISS) and transmission electron microscopy (JEM 1200 EXII JEOL). Specific surface area measurements were performed using ASAP 2010 M instrument (Micromeritics). The percentage content of the materials was determined by the elemental analysis of C, H, N, S (vario MICRO cube, Elementar Analysensysteme GmbH). The particle size distribution were determined by Mastersizer S (Malvern).

2.2 Electrochemical measurements

The electrochemical performance of symmetric and asymmetric capacitors was studied in two and three electrode Swagelok® systems, using 1M Na_2SO_4 aqueous solutions as electrolyte. Electrodes contained 85% of active material, 10% of binder (PVDF, Kynar Flex 2801) and 5% of acetylene black (to ensure good conductivity). In case of asymmetric systems, composite materials have been selected for a positive electrode while activated carbon obtained by carbonization of lignin (AC1) was a negative one. The capacitance properties were studied by three electrochemical techniques: cyclic voltammetry ($1 – 100$ mV s^{-1}), galvanostatic charging/discharging (100 mA g^{-1} – 10 A g^{-1}) and electrochemical impedance spectroscopy (100 kHz – 1 mHz) using potentiostat/galvanostat VMP3/Z (Biologic, France). All capacitance values are expressed per one electrode; in case of asymmetric configurations average mass was taken into account.

3. RESULTS AND DISCUSSION

C/MnO_2 composites with different carbon materials were prepared with various MnO_2 content (c.a. 30, 50 and 60% of MnO_2). Labeling, composition and BET surface area of the composites are

shown in Table 1. For more detailed study carbon materials of different structure and porosity as well as different specific surface area were used as it might be stated from Table 1.

Table 1. Composition of materials (percentage content determined by elemental analysis of C, H, N, S) and the specific surface area.

Labelling of the composite	Type of carbon	Carbon content [%]	MnO_2 content [%]	BET surface area [$m^2\ g^{-1}$]
AC1	Activated Carbon	100	-	2904
AC2	Norit GSX	100	-	836
DN	MWNTS 110-170	100	-	18
MN	MWNTS 7-15	100	-	305
MnO_2	-	-	100	116
AC2 MnO_2 1	Norit GSX	60	40	475
AC2 MnO_2 2	Norit GSX	49	51	305
AC2 MnO_2 3	Norit GSX	39	61	280
DN MnO_2 1	MWNTS 110-170	66	34	47
DN MnO_2 2	MWNTS 110-170	53	47	96
DN MnO_2 3	MWNTS 110-170	40	60	120
MN MnO_2 1	MWNTS 7-15	67	33	191
MN MnO_2 2	MWNTS 7-15	48	52	164
MN MnO_2 3	MWNTS 7-15	38	62	90

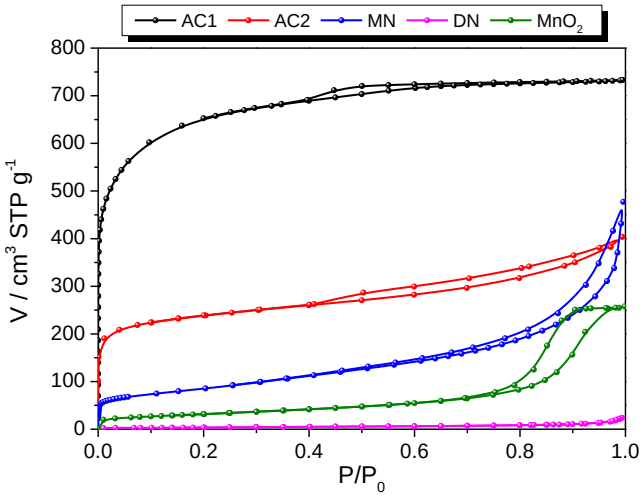

Figure 1. N_2 adsorption/desorption isotherms (77 K).

Structural differences originating from the nature of the materials can be seen also in Fig. 1 showing the BET adsorption isotherms. The shape of the curves indicates the different nature of the

pores in the selected carbon materials from micro- (AC1, AC2) through meso- (MN) to macropores (DN). The profile of the adsorption isotherm with hysteresis loop for MnO_2 indicates the presence of mesopores. In case of electrode materials for electrochemical capacitors, well-developed surface area significantly affects the growth of capacitance, by forming the electrical double layer at the electrode/electrolyte interface. However, the size and shape of the pores affect the transport of ions, hence the contribution of mesopores is necessary in order to receive good charge propagation.

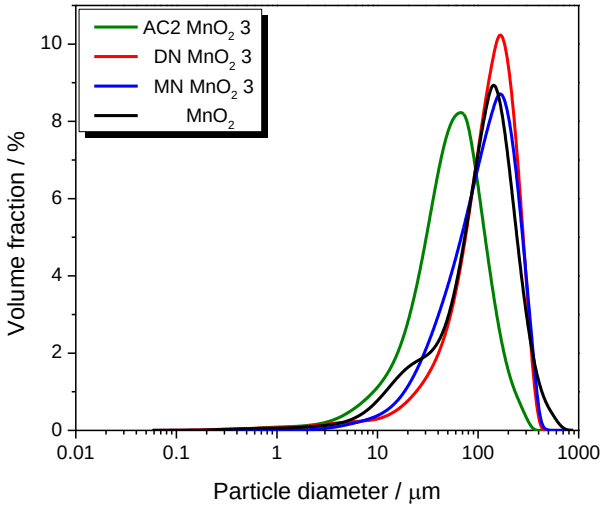

Figure 2. Particle size distribution.

Fig. 2 shows the particle size distribution of the composite materials with the highest content of manganese dioxide (c.a. 60%), and for comparison of pure MnO_2. AC2 MnO_2 3 having an average particle size of about 50 μm differs from other materials, with an average size of about 200 μm. This can be caused by structural differences of carbonaceous materials because carbon nanotubes mostly form the compact structure (Fig. 5). An example of X-ray structural analysis shown in Fig. 3. Diffraction patterns recorded for DN and their composites with MnO_2 present well-developed peak at 26° 2θ derived from carbon of an ordered structure. The intensity of this peak decreases with increasing content of manganese dioxide. On the spectrum do not appear peaks originating from MnO_2, what indicates amorphous form as expected during preparation.

The surface morphology of the source materials are shown in Fig. 4 and Fig. 5. There is an apparent difference in the selected materials. MnO_2 has the form of irregular grains resembling tiny crystals. Activated carbon AC1 has a spherical shape, mostly fragmented into smaller components resembling inside cheese with large holes, whereas the appearance of bee combs can be attributed to AC2. Completely different structure have a carbon nanotubes (Fig. 5). In this case, it is difficult to separate the individual particles, since they have compacted and twisted structure, similar in shape to the sea sponges or corals. Examples of SEM and TEM images of composite materials contains in Fig. 6. As can be seen pure MnO_2 has the form of fine particles deposited on the surface of a variety of carbon materials.

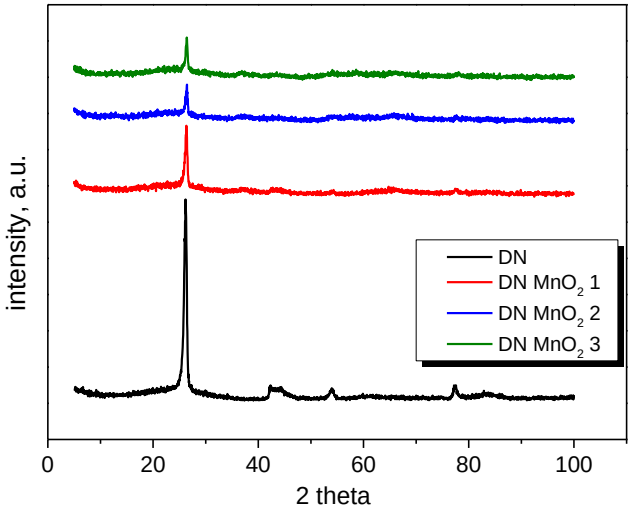

Figure 3. Diagram of X-ray diffraction.

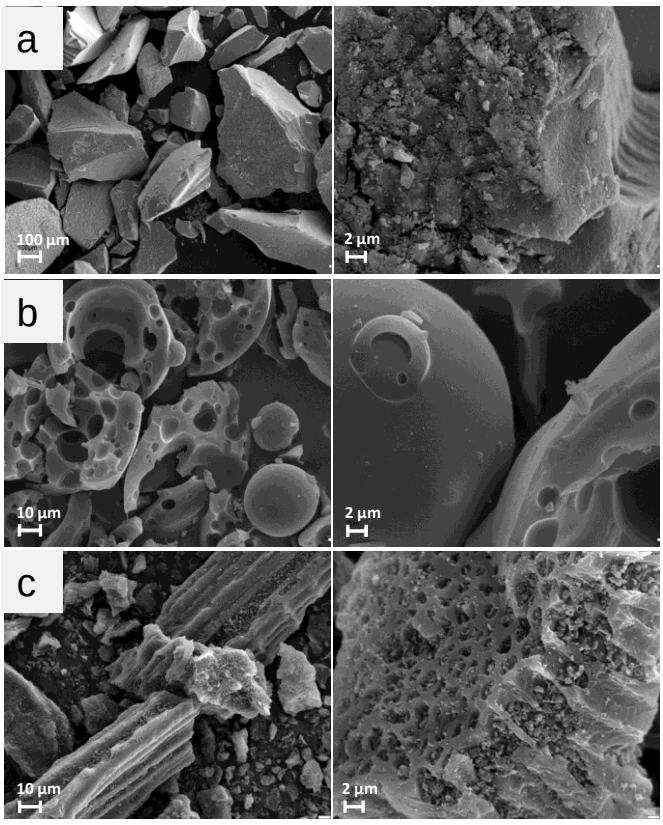

Figure 4. SEM images of MnO_2 (a) AC1 (b) and AC2 (c).

The first stage of the electrochemical study included the determination of capacitance characteristics for source materials and produced composites in symmetrical systems. In preliminary tests, the highest capacitance values were obtained for composites with 60% of MnO_2. Carbon materials also showed differences in the energy storage ability.

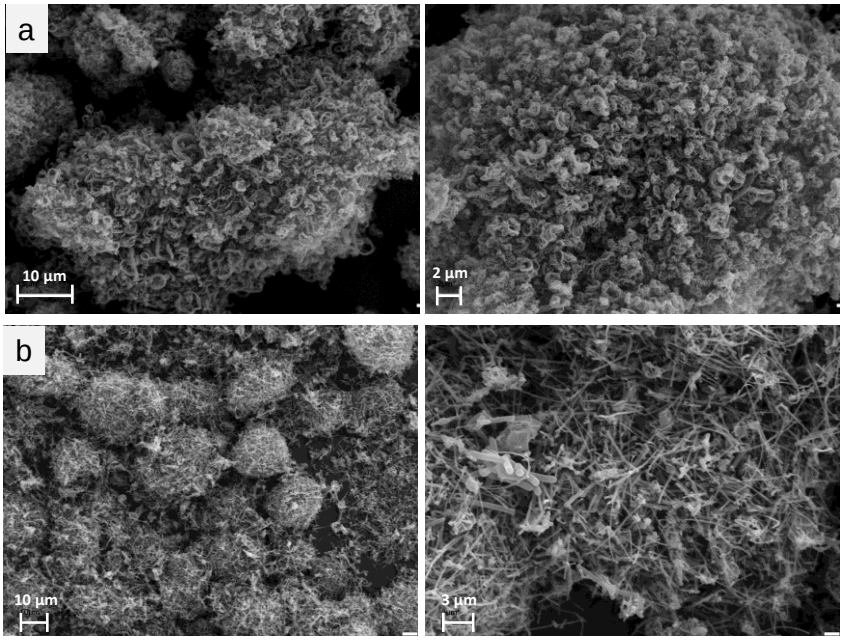

Figure 5. SEM images of MN (a) and DN (b).

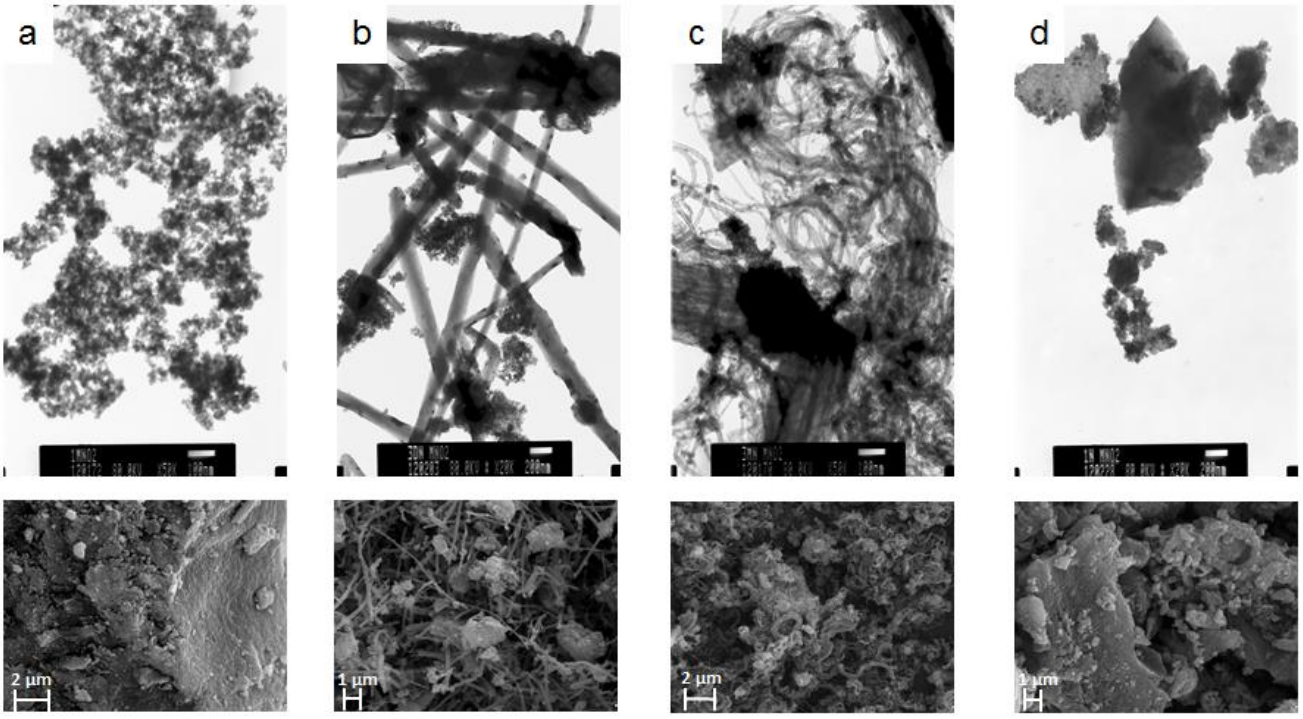

Figure 6. TEM and SEM (bellow) images of MnO_2 (a), DN MnO_2 3 (b), MN MnO_2 3 (c) and AC2 MnO_2 1 (d).

Fig. 7 shows the relationship between capacitance and voltage of carbons used for research, and of MnO_2. The highest capacitance values were obtained for the carbon AC1 having the most developed surface area (2904 $m^2 g^{-1}$). Capacitance for both carbon nanotubes and activated carbon AC2 was significantly lower compared to the carbon AC1, therefore, they were used as materials

improving the conductivity of MnO_2. The electrochemical characterization of composite materials with the most favorable composition, depict Figs. 8, 9, 10. Studies carried out with three electrochemical techniques have shown that the material with the highest capacitance is a composite of MnO_2 with AC2 (AC2 MnO_2 3), while the worst performance was obtained for DN composite (DN MnO_2 3). Results for MN MnO_2 3 were similar to those obtained for AC2 MnO_2 3, although for galvanostatic charging/discharging with current regime of 10 A g^{-1} higher capacitance value was observed for capacitor with MN MnO_2 3 (Fig. 9). Frequency response presented in Fig. 10 reveals sharp decrease in capacitance in the range from 1 mHz to 1 Hz, reflecting the deterioration of the charge propagation with the increase of the frequency regime.

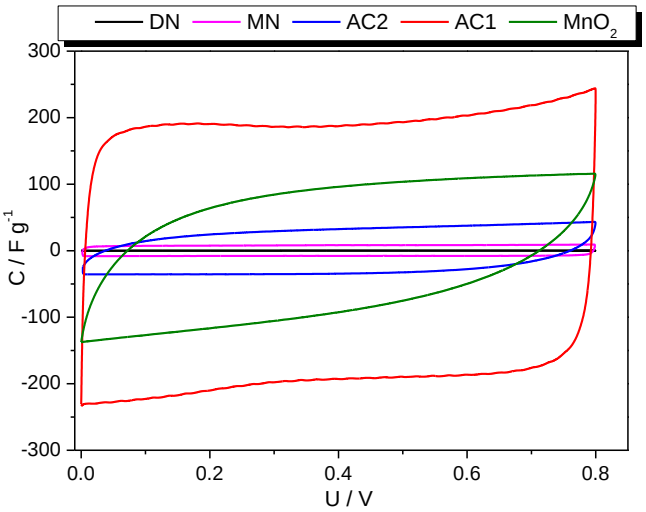

Figure 7. Cyclic voltammetry curves recalculated prior scan rate of selected carbon materials and pure manganese dioxide. Scan rate10 mV s^{-1}.

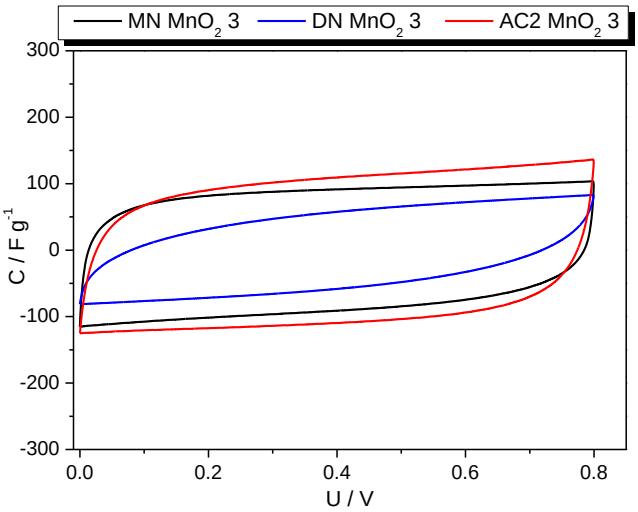

Figure 8. Cyclic voltammetry curves recalculated prior scan rate of composite materials with ca. 60% MnO_2. Scan rate10 mV s^{-1}.

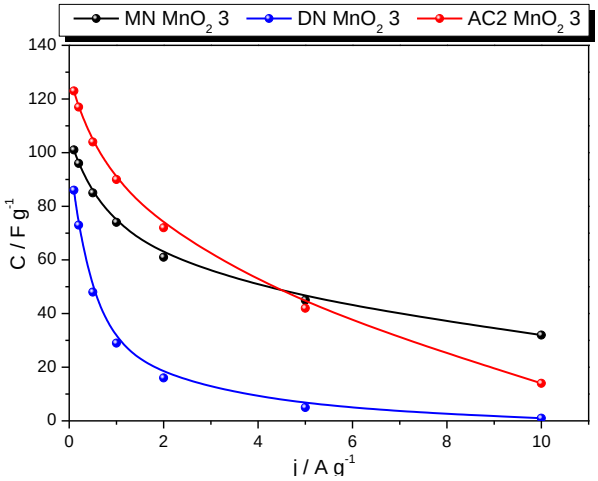

Figure 9. The relationship between capacitance and current density for composite materials with the highest content of MnO_2.

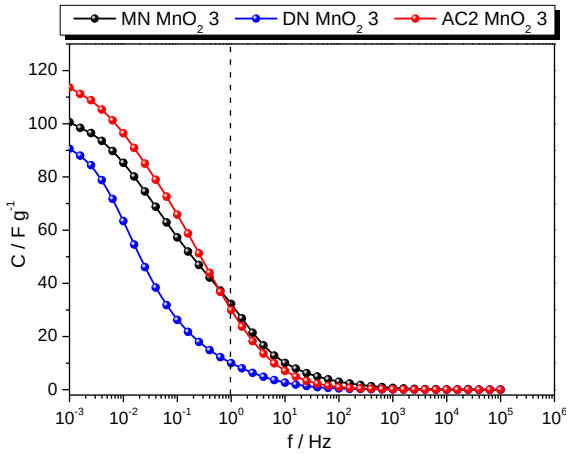

Figure 10. Capacitance vs. frequency dependence for composite materials with 60% of MnO_2.

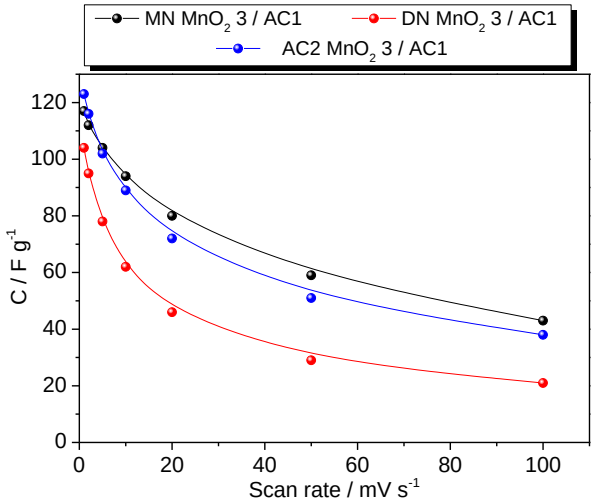

Figure 11. The relationship between capacitance and scan rate for asymmetric capacitors.

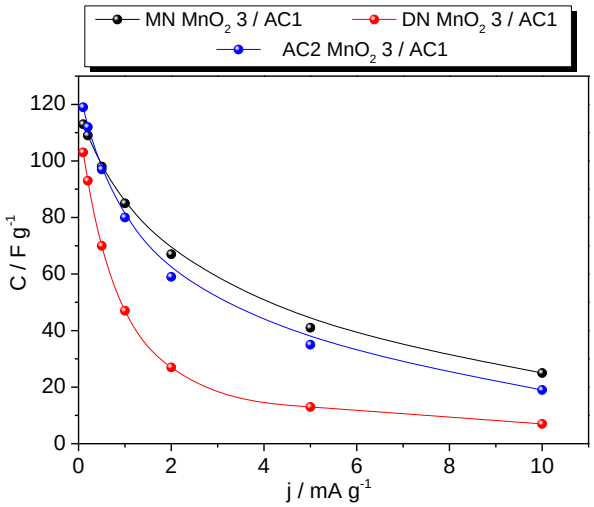

Figure 12. The relationship between capacitance and current density for asymmetric capacitors.

Fig. 11 and Fig. 12 summarizes the capacitance values calculated from cyclic voltammetry and galvanostatic charging/discharging for asymmetric systems built of composites containing 60% MnO_2, operating at a voltage of 0.8 V. The best results were obtained for the AC2 MnO_2 3/ AC1 and MN MnO_2 3/ AC1 systems. Nevertheless, the differences between the capacitance values in both cases were not significantly large, but merely at the level of ca. 10 Farad per gram.

Operating voltage for all three systems were extended over the range of thermodynamic stability of water (1.23 V). The study was performed using cyclic voltammetry at a scan rate of 10 mV s^{-1}. The capacitor constructed of composite AC2 MnO_2 3 gave most preferred capacitance at the level 142 F g^{-1} in the extended voltage range (1.7 V), which is much higher comparing to 95 F g^{-1} in standard conditions for aqueous electrolytes (0.8 V) (Fig. 13c). Other configurations also showed an increase in capacitance with the extension of the operating voltage although the increase was comparatively smaller. Examples of capacitance dependence of asymmetric capacitors calculated from voltammetric curves posted in Figure 13. The tests were performed in a two-electrode configuration (Fig. 13a, 13b, 13c), and a three-electrode configuration (Fig. 13d, 13e, 13f) recording the behavior of the individual electrodes. A parameter determining the operating range of the asymmetric capacitor is the potential of decomposition of the electrolyte. This feature depends on the composition and the type of electrode material. In the case of two-electrode system recorded curves are quite similar irrespective of kind of composite or C:MnO_2 proportions. More useful, and giving more information are measurements in three-electrode cells. This kind of study, allows to observed the processes of oxygen or hydrogen evolution resulting from the decomposition of water in the electrolyte. Consequently, based on observations of the system as a whole, the capacitor voltage can be determined to approximately 1.6 V for the MN MnO_2 2 and MN MnO_2 3 composites, and for AC2 MnO_2 3 maximally to 1.2 V. Considering each electrode separately (three electrodes test), the potential of electrodes polarization constitutes 1.2 V, for all presented samples.

(a)

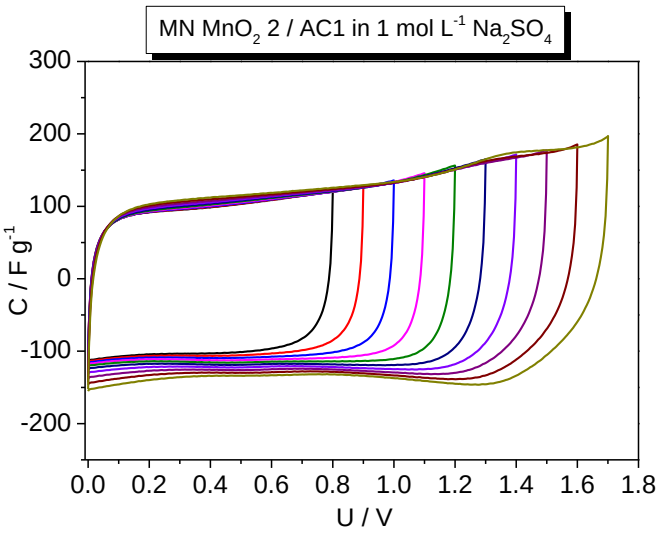
MN MnO2 2 / AC1 in 1 mol L-1 Na2SO4
C / F g-1
U / V

(b)

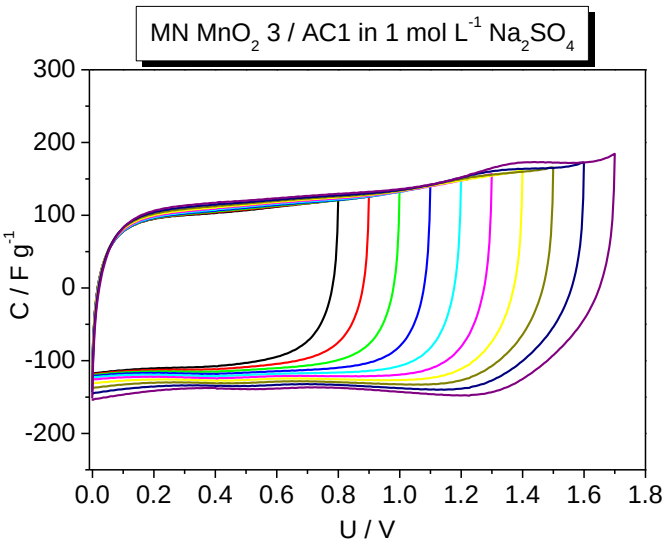
MN MnO2 3 / AC1 in 1 mol L-1 Na2SO4
C / F g-1
U / V

(c)

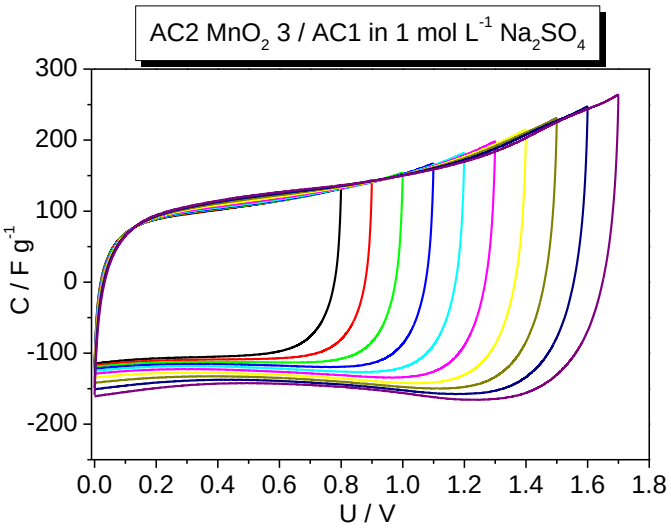
AC2 MnO2 3 / AC1 in 1 mol L-1 Na2SO4
C / F g-1
U / V

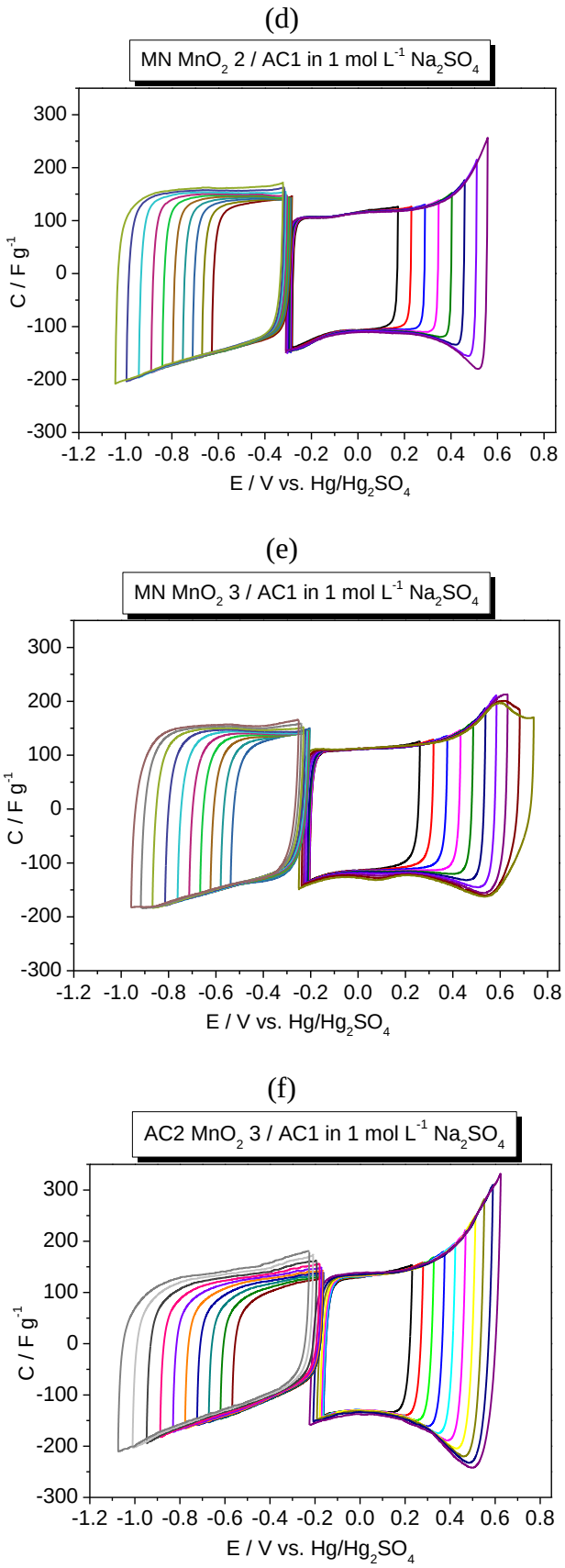

Figure 13. Capacitance dependence calculated from cyclic voltammetry for asymmetric capacitors in a two-electrode system recorded at a scan rate of 10 mV s^{-1} (left), and three-electrode system recorded at 5 mV s^{-1} (right).

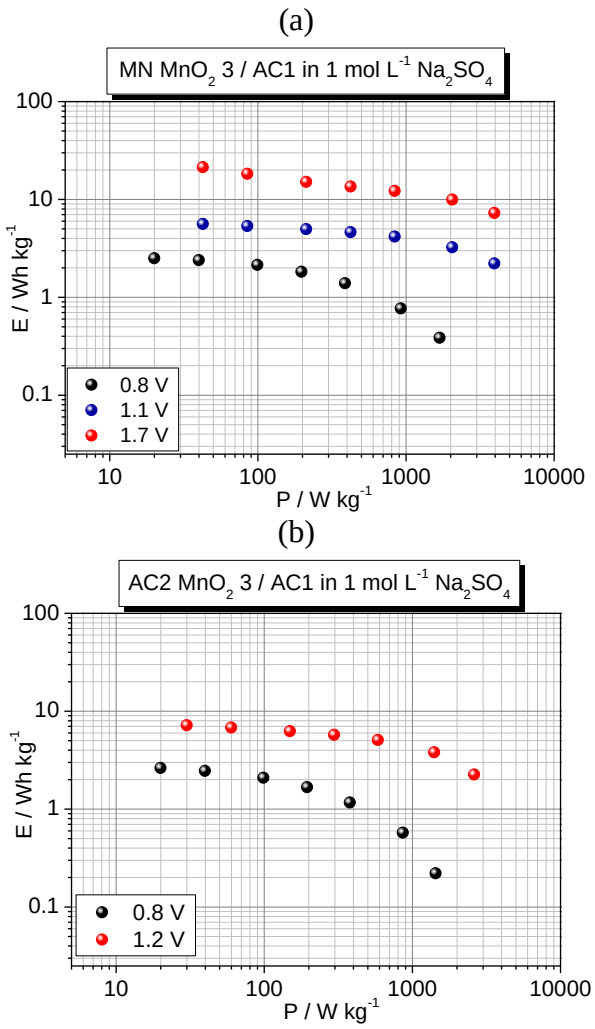

Figure 14. Ragone plots for the asymmetric capacitors operating in different voltage ranges (from 0 V).

Fig. 14 shows diagrams describing power-energy dependence for asymmetric systems operating in standard (0.8 V) and extended voltage range. The best results were obtained for the MN MnO_2 3/ AC1 cell but for all presented examples can be seen enhancement of power and energy density by increasing the operating voltage. The capacitor MN MnO_2 3/ AC1 operating at a voltage of 1.7 V reached energy density above 20 Wh kg^{-1}. Comparison of the power-energy efficiency of symmetric and asymmetric capacitors presents Ragone graph in Fig. 15. Pure MnO_2 shows a sharp decline in energy density at the expense of increasing the power of such a system. The improvement in power performance, while maintaining the same level of energy gave the formation of manganese dioxide composite with carbon nanotubes (MN). In case of carbon AC1 power-energy dependence is nearly linear relation on the energy density level around 5 Wh kg^{-1}.

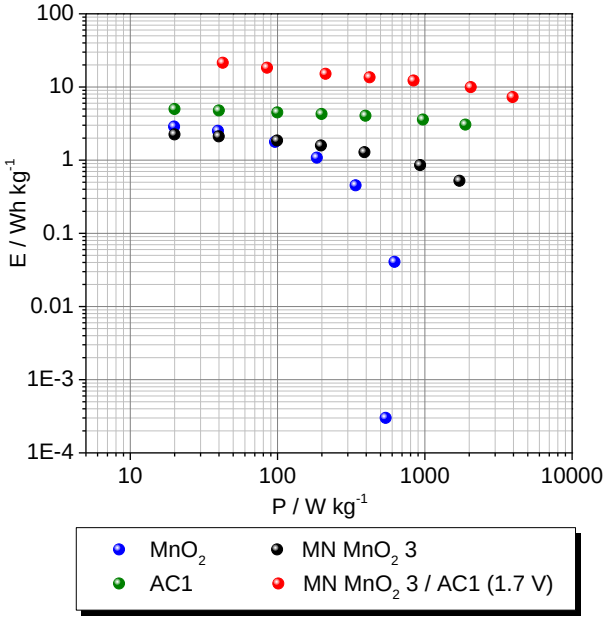

Figure 15. Ragone plot for the symmetric capacitors: MnO_2/ MnO_2, MN MnO_2 3/ MN MnO_2 3, AC1/ AC1 and for the asymmetric capacitor MN MnO_2 3/ AC1 working at a voltage of 1.7 V.

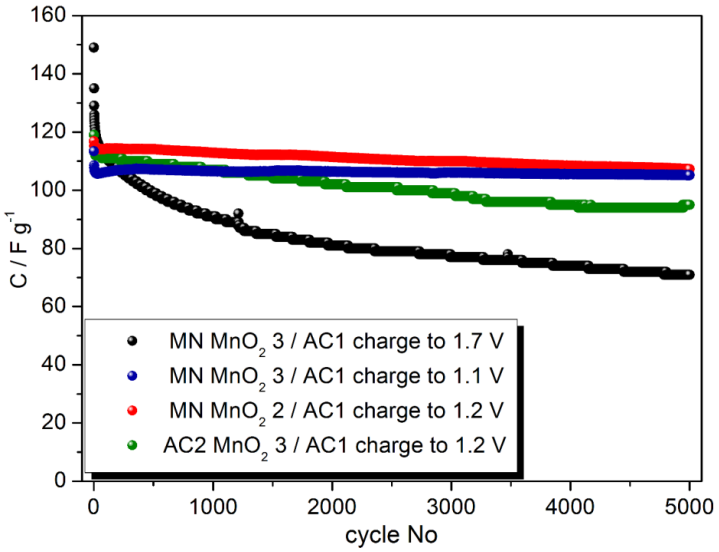

Figure 16. Cycle performance of asymmetric cells in the extended operating voltage range. Load current density: 2 A g^{-1}.

The increase of energy stored in electrochemical capacitors is important from the point of application. However, cyclic performance of such systems should be also take into account. Fig. 16 shows cyclic performance of electrochemical capacitors built of composites containing carbon nanotubes and MnO_2 (50% and 60% of MnO_2), and the composite of the carbon AC2 with MnO_2 (60%). Very good stability during 5000 cycles were obtained for composites MN MnO_2 charged to 1.1 V (blue balls) and 1.2 V (red balls). The capacitance of these systems has remained at around 110 F g^{-1} at a load current density 2 A g^{-1}. Increase of operating voltage of the capacitor MN MnO_2 3/ AC1 from

1.2 V to 1.7 V, initially has contributed to increase in capacitance, although during 5000 cycles quite significant fall from ca. 150 F g^{-1} to ca. 70 F g^{-1} was observed. Apparent capacitance decrease during cyclic work from approximately 120 F g^{-1} to 95 F g^{-1} can also be observed for the material AC2 MnO_2 3 (green balls). Wrong selection of operating voltage range which can cause the decomposition of the electrolyte can result in a significant loss of capacitance during cyclic work. In the literature results with similar systems can be found, however, they cannot be compared in a direct way. Obtained values of both energy and capacitance are dependent on the method of manganese dioxide synthesis, the type of the carbon skeleton, and the properties of the carbon used as a negative electrode, as well as kind of electrolyte.

Tomko *et al.* received energy density approximately 20 Wh kg^{-1} at a power density of 1 kW kg^{-1} for asymmetric aqueous electrochemical capacitors, using for fabrication high surface area carbon derived from coal tar pitch and manganese dioxide. During 1000 cycles of galvanostatic charging/discharging at a load current density 1.5 A g^{-1} and a cell voltage of 2 V, the resulting capacitance was between 35 and 45 F g^{-1} [17]. Similar results were obtained by Deng *et al.* for composite graphene/multiwall carbon nanotubes/MnO_2. Asymmetrical capacitor gave a high energy density of 28 Wh kg^{-1} at a cell potential of 2 V. However, the capacitance of such a system during the 2500 cycles was maintained at a level below 30 F g^{-1} at a current density of 1 A g^{-1} [7]. Another example is the paper of Gao *et al.* which reports that the capacitance of activated carbon (AC)/ MnO_2 - AC system reached 33 F g^{-1} in operating window of 2 V and after 2500 cycles maximum energy density was 18 Wh kg^{-1} [19]. Most of the examples in the literature presents the energy density of approximately 25 - 35 Wh kg^{-1} for asymmetric capacitors with a voltage range 2 V, although the capacitance of such systems rather do not exceed 60 F g^{-1} during long term cyclic work [20-22]. Examples which show higher values of capacitance are rather related with symmetric capacitors, working at narrower voltage range. For MnO_2/ graphene foam composite in the range 0.5 V (starting from 0 V) at the current density of 0.2 A g^{-1}, obtained capacitance was 560 F g^{-1}. During 1000 cycles this value decreased of about 21% [23]. At slightly higher voltage, i.e. of 0.6 V, another research group received capacitance above 150 F g^{-1} (200 cycles, current 0.1 A g^{-1}). Investigated material was composite of MnO_2 with carbon nanotubes [24]. Other studies, also for composite with carbon nanotubes, gave the capacitance of ca. 171 F g^{-1} (voltage range 0 - 0.8 V). In this case, current load was 1 A g^{-1}, what is significantly higher value [25]. The following examples show that a variety of results for seemingly the same materials can be obtained. They also show the possibility to control such systems in order to optimize their work in terms of power - energy efficiency. In this paper, authors presented the results of studies carried out for the asymmetric capacitors built from composites of carbon and MnO_2, showing moderate capacitance values accompanied by extended operating voltage of considered systems.

4. CONCLUSIONS

Composites of carbon materials and MnO_2 have been examined by three electrochemical techniques in symmetric and asymmetric systems as a positive electrode materials. The asymmetric

configuration of materials of different nature gave a significant increase in the operating voltage. The combination of two different electrode materials with varying energy storage mechanism, allow for extension of operating voltages by using an aqueous electrolyte. This involves to the change the hydrogen evolution overpotential causing electrolyte decomposition. Taking into account the use of the composite of manganese dioxide as a positive electrode material to increase the operating voltages, it should be remembered that each of the electrodes gives a different answer to expansion of operating voltage, so it should be viewed not only as a whole but also separately. Excessive expansion of the voltage window in order to increase the acquired energy density can contribute to a significant decrease in the capacitance of such a system. Cyclability of the systems presented in this paper is acceptable, if voltage value does not exceed 1.2 V.

ACKNOWLEDGEMENTS
The authors acknowledge the financial support from the European Fund of Regional Development within the frameworks of the operating program –"Innovative Economy 2007–2013", under Project No. POIG.01.01.02-00-015/09.

References

1. M. Winter, R.J. Brodd, *Chem. Rev.*, 104 (2004) 4245
2. A. Burke, *J. Power Sources*, 91 (2000) 37
3. J. Miller, P. Simon, *Science*, 321 (2008) 651
4. L. Deng, Z. Hao, J. Wang, G. Zhu, L. Kang, Z-H. Liu, Z. Yang, Z. Wang, *Electrochim. Acta*, 89 (2013) 191
5. S.H. Li, Q.H. Liu, L. Qi, L.H. Lu, H.Y. Wang, *Chin. J. Anal. Chem.*, 40 (3) (2012) 339
6. S.H. Kim, Y.I. Kim, J.H. Park, J.M. Ko, *Int. J. Electrochem. Sci.*, 4 (2009) 1489
7. L. Deng, Z. Hao, J. Wang, G. Zhu, L. Kang, Z.H. Liu, Z. Yang, Z. Wang, *Electrochim. Acta*, 89 (2013) 191
8. Y. Qian, S. Lu, F. Gao, *J. Mater. Sci.*, 46 (2011) 3517
9. X. Dong, X. Wang, J. Wang, H. Song, X. Li, L. Wang, M.B. Chan-Park, C.M. Li, P. Chen, *Carbon*, 50 (2012) 4865
10. P. Simon, Y. Gogotsi, *Nat. Mater.*, 7 (2008) 845
11. B.E. Conway, V. Birss, J. Wojtowicz, *J. Power Sources*, 66 (1997) 1
12. J.W. Long, D. Belanger, T. Brousse, W. Sugimoto, M.B. Sassin, O. Crosnier, *MRS Bull*., 36 (2011) 513
13. C. Shen, X. Wang, S. Li, J. Wang, W. Zhang, F. Kang, *J. Power Sources*, 234 (2013) 302
14. C.C. Hu, T.W. Tsou, *Electrochem. Commun.*, 4 (2002) 105
15. F. Xiao, Y. Xu, Int. *J. Electrochem. Sci.*, 7 (2012) 7440
16. T. Brousse, P.L. Taberna, O. Crosnier, R. Dugas, P. Guillemet, Y. Scudeller, Y. Zhou, F. Favier, D. Belanger, P. Simon, *J. Power Sources*, 173 (2007) 633
17. T. Tomko, R. Rajagopalan, M. Lanagan, H.C. Foley, *J. Power Sources*, 196 (2011) 2380
18. F. Lufrano, P. Staiti, E.G. Calvo, E.J. Juarez-Perez, J.A. Menendez, A. Arenillas, *Int. J. Electrochem. Sci.*, 6 (2011) 596
19. P.C. Gao, A.H. Lu, W.C. Li, *J. Power Sources*, 196 (2011) 4095
20. X. Zhang, X. Sun, H. Zhang, D. Zhang, Y. Ma, *Mater. Chem. Phys.*, 137 (2012) 290
21. C.J. Jafta, F. Nkosi, L. le Roux, M.K. Mathe, M. Kebede, K. Makgopa, Y. Song, D. Tong, M. Oyama, N. Manyala, S. Chen, K.I. Ozoemena, *Electrochim. Acta*, 110 (2013) 228

22. L.F. Chen, Z.H. Huang, H.W. Liang, Q.F. Guan, S.H. Yu, *Adv. Mater.*, 25 (2013) 4746
23. X. Dong, X. Wang, J. Wang, H. Song, X. Li, L. Wang, M.B. Chan-Park, C.M. Li, P. Chen, *Carbon*, 50 (2012) 4865
24. E. Raymundo-Pinero, V. Khomenko, E. Frackowiak, F. Beguin, *J. Electrochem. Soc.*, 152 (2005) A229
25. R. Jiang, T. Huang, Y. Tang, J. Liu, L. Xue, J. Zhuang, A. Yu, *Electrochim. Acta*, 54 (2009) 7173